Tunable Coaxial Bandpass Filters Based on Inset Resonators

Abdulrahman Widaa, *Graduate Student Member, IEEE*, Chad Bartlett, *Graduate Student Member, IEEE*, and Michael Höft, *Senior Member, IEEE*

***Abstract*—A new class of compact, high-Q, tunable coaxial filters is presented in this paper based on a novel inset resonator concept. The tuning concept is based on the displacement of movable resonators inside a properly modified metallic housing which features wide tuning capabilities and stable high Q-factor performance with minimum variation throughout the tuning window. Various prototypes are designed and implemented to demonstrate and validate the proposed concept. A single tunable inset resonator is first designed and measured showing distinctive results of a 43% tuning range, stable high-Q of 4100±4%, spurious-free band up to 3.8·f_0, and volume-saving up to 50% when compared to the conventional combline and half-wavelength structures. The design procedure for constant absolute bandwidth (CABW) tunable filters is then presented, and two different tunable inset filters are designed and implemented. Firstly, a manually tunable four-pole filter is demonstrated with the merits of a wide 39.3% tuning range, while maintaining a constant bandwidth of 116 MHz±6%, and a stable high-Q of 1820±6%. Next, an automatically tunable 3rd-order inset filter is designed and measured using high-accuracy piezomotors. Similarly, the measured results exhibit a wide 1.3 GHz tuning range from 2.65 GHz - 3.95 GHz with a stable insertion loss that is less than 0.35 dB, a return loss that is better than 15 dB, and a good spurious performance up to 2.8·f_0. To our own knowledge, the proposed tuning technique and tunable components represent state-of-the-art tuning range and stable high-Q with minimal variation when compared with similar loaded-waveguide designs.**

***Index Terms*—Constant bandwidth, inset filter, miniaturization, passive components, tunable filters, waveguide technology.**

I. Introduction

PROPELLED by the exponential development in the telecommunication industry and the escalating demand for more efficient and adaptable multi-channel multi-standard systems, tunable microwave filters are constantly gaining ground as they are playing a pivotal role in frequency-agile RF front-ends and payloads. The tunable filter market is expected to have an annual growth of more than 10%, crossing USD 148 million by 2025 [1], driven mainly by major industrial sectors including RADAR systems, test and measurement instruments, and software-defined radios. These evolving applications have stringent requirements for high-performance tunable filters with regard to volume and mass, high unloaded quality factor (Q_u), and wide tuning capabilities with efficient tuning mechanisms. Looking in the available literature, tunable filters have been realized in planar and 3-dimensional structures using a variety of different electrical, magnetic, and mechanical tuning means [2]. While the majority of research is based on simple, compact, and low-cost planar tunable microstrip filters which utilize fast electrical tuning elements (e.g., varactor diodes) [3], their high losses and poor power performance hinder their employment in high-performance applications. On the other hand, the use of waveguide filters, despite their high Q-factor and ability to handle high power levels, usually have bulky structures, as well as slow and narrow tuning capabilities (<5% tuning) [4], making hollow waveguide tunable filters an unfavorable solution; especially at lower frequency bands less than 10 GHz. Considering the drawbacks of the aforementioned technologies, loaded-waveguide structures have attracted more attention in tunable filters applications due to being much more compact when compared with hollow waveguide designs, while still providing comparably high quality factors. Accordingly, various loaded-waveguide tunable filter designs were presented based on dielectric resonators, conventional metallic half-wavelength, and combline configurations using

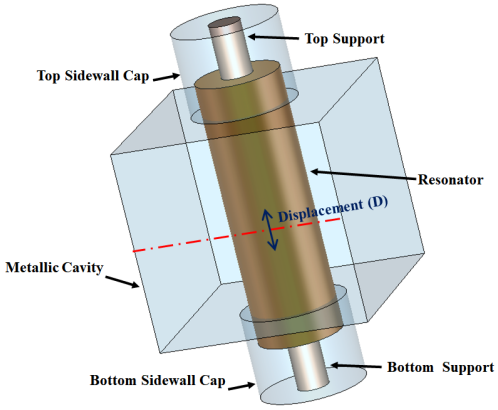

Fig. 1. Perspective view of the inset resonator configuration. Tunable responses are obtained through the displacement of the movable resonator inside modified parts of the cavity (caps). The resonant frequency is the lowest when the resonator in centred (D=0) and increases gradually when $|D| > 0$.

Manuscript received XX XX, 2022; Revised XX XX, 2022; Accepted XX XX, 2022. This project has received funding from the European Union's Horizon 2020 research and innovation programme under the Marie Skłodowska-Curie grant agreement 811232-H2020-MSCA-ITN-2018.

This article is an expanded version from the 2022 International Microwave Symposium, Denver, CO, USA, June 19–24, 2022 [DOI: 10.1109/IMS37962.2022.9865311]. *(Corresponding author: Abdulrahman Widaa.)*

A. Widaa, C. Bartlett and M. Höft are with the Department of Electrical and Information Engineering, Kiel University, Kiel 24118, Germany (e-mail: aw,chb,mh@tf.uni-kiel.de).

Color versions of one or more of the figures in this article are available online at http://ieeexplore.ieee.org.

Digital Object Identifier XXX/TMTT.XXXX

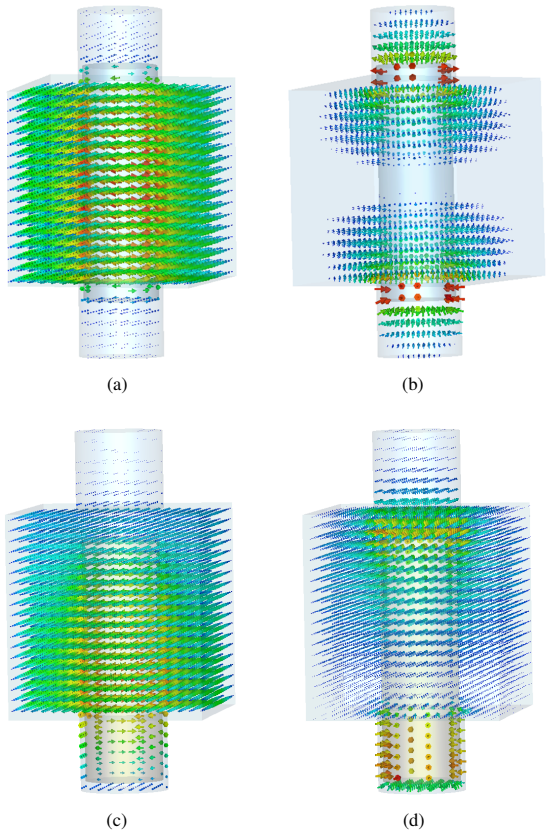

Fig. 2. Fields distribution inside the inset resonator at the extreme ends of the tuning range. (a). H-field, (b) E-field at the lowest tuning state. (c). H-field, (d) E-field at the highest tuning state.

different mechanical tuning means [5]- [20]. A 2.5 GHz tunable $\lambda/2$ coaxial filter was presented in [5] with a 20% tuning range by using a common element which rotates all of the resonators simultaneously inside an elliptical cavity, providing a means of tuning the operation frequency. However, this mechanism of tuning has limited tuning capabilities since it functions only within a specific range of the cavity (0° - 90°). Furthermore, the filter experiences a noticeable deterioration in the Q-factor (≈20%) when the resonators are rotated closer to the cavity, which ultimately increases the losses. The large size, and degraded spurious responses are further drawbacks of this half-wavelength configuration. According to the authors' knowledge, this is the only tunable filter available in the literature based on the conventional $\lambda/2$ resonators. On the other hand, several combline-based tunable filters were presented using different tuning elements and means [6]- [13], [18]- [20]. A straightforward approach is by using mechanically, vertically movable tuning screws, disks, or sidewalls in the vicinity between the combline resonators and the top part of the metallic cavity [6]- [10]. For example, [7] introduced an 18% reconfigurable S-band combline filter using dielectric tuning posts controlled by a common tuning plate. Also in [9], a 2.6 GHz $\lambda/4$ tunable coaxial combline filter was implemented using metallic tuning discs controlled by individual piezomotors with a very small tuning range (≈70 MHz). A third example employing a piezoelectrically-actuated flexible sidewall was presented in [10]. A four-pole C-band tunable dielectric combline filter is implemented with 4% tunability and unloaded Q-factor of less than 550. In this regard, it is clear that this category of vertically movable tuning elements suffers from severe deterioration in the Q_u as the tuning elements approach closer to the combline resonators, with additionally risking the possibility of generating unwanted spurious resonances. Excellent electrical contact must be guaranteed between the top part of the cavity and the tuning elements (i.e. using nuts), otherwise, the Q-factor will be impacted negatively and the tuning range will decrease. Besides, the volume of such filters is relatively large since the height of the cavity must be increased to provide room for the tuning screws/disks inside of the housing. Another group of tunable coaxial combline filters is employing horizontally sliding and/or rotational metallic or dielectric elements mounted on a common tuning post [11]- [13]. For instance, an L-band tunable $\lambda/4$ combline filter was introduced in [12] with an 11% tuning range using rotational elliptical metallic loadings. In comparison with the aforementioned group of vertically movable tuning elements, this configuration features an easier tuning process. However, the frequency tuning windows of these means are very narrow since less EM field can be perturbed. Hence, larger elements must be used to increase the tuning capabilities. Unfortunately, this increases the size and weight of the filter and also unwanted spurious resonances might appear. Recently, we presented tuning concepts based on TM-mode dielectric resonators featuring compact structures and wide tuning capabilities >90% [14]- [17]. Unfortunately, they also experience noticeable deterioration in the Q_u with the tuning process. Besides the above mechanical-based tuning technique which is the most favorable, couple of loaded-waveguide filters were introduced using electrical and magnetic tuning elements to attribute fast tuning speed [18]- [20]. For example, the authors in [18] presented reconfigurable 2nd-order dielectric filters using tuning circuits loaded with MEMS and GaAs varactors. The filters show tuning windows up to 3.5% with an unloaded quality factor ranging from 170 to 1220. Similarly in [19], 30% varactor-tuned combline filters were implemented with a quality factor of 173 to 418. Also, a two-pole L-band ferrite-loaded tunable combline filter was introduced in [20] with 41% tunability and a Q_u varies from 1223 to 2425. It can be shortly said that both electrical and magnetic tuning means still need more development to be employed effectively in tunable waveguide filters and compete with the mechanical-based tuning techniques. Many major challenges must be addressed further including the losses, power handling capabilities, and integration complexity.

Given all these aforementioned limitations and challenges of the various state-of-the-art designs, the introduction of more efficient tuning mechanisms and tunable filter structures is thoroughly required. This work presents new tunable filter designs based on our novel so-called *inset* resonator configuration which was briefly introduced in [21] for both fixed and tunable filter applications. Compared to the conventional half-wavelength and combline structures, the proposed inset topology advantageously features more compact structures, enhanced spurious performance, and comparably similar Q-factors. Additionally, tunable inset filters and components can

be designed effectively with wide, extended frequency tuning capabilities while maintaining a stable Q_u that have only minimal deterioration over the specified tuning range.

In the following sections, the tunable inset resonator configuration is first introduced and detailed. Then, the design procedure of tunable filters with constant absolute bandwidth (CABW) is discussed, and tunable inset filters are designed and implemented using different realization setups. Measurements are discussed and a detailed comparison with similar state-of-the-art tunable filters is provided with a discussion and followed by a conclusion.

II. Tunable Inset Resonator Configuration and Operating Principle

A. Structure and Setup

The inset resonator setup is depicted in Fig. 1. It comprises a metallic or dielectric resonator inserted partially inside a metallic housing with modified sidewalls (caps). The resonator is positioned within the cavity using a support made of a low-loss material (e.g. Teflon, Rexolite) and has neither electrical nor mechanical contact with the metallic housing. As shown in [21], the inset resonator configuration has highly desirable advantages in comparison with the conventional half-wavelength and combline structures, including more compactness, better spurious performance, and comparably high Q-factor with the best Q_u/volume ratio. As can be seen in Fig. 2, the inset resonator initially operates using the fundamental TM mode with a half-wave field distribution similar to the conventional $\lambda/2$ structures. Here, due to the capacitive load at both cap-ends, the length of the resonator can be shortened substantially (>50%). The dominant magnetic field is mainly resonating in the middle, while the electric field is maximum at the ends of the resonator and minimum in the middle. Accordingly, the current density is minimum at the ends of the resonator and a relatively low current density is present along the housing sidewalls. This advantageously results in a higher Q-factor for the overall resonator assembly. Furthermore, the sidewall caps are designed to contain the lowest field intensities, therefore, the high Q-factor can be maintained even when there is a close proximity between the resonator and sidewall caps [21]. It is also worth mentioning that in addition to the configuration in Fig. 1, other shapes of resonators and sidewall caps can be used (e.g. conical), and alternative arrangements can be realized following the same concept of the design but have different performance characteristics [22].

B. Operation Principle

By looking back at the available literature, it can be concluded that there are three major challenges that tunable filter designers are concerned with:

- how to design compact tunable structures that are able to provide wide tuning ranges,
- how to have a tunable structure without the need for auxiliary tuning elements (e.g. screws, disks),

and

- how to maintain a high, yet stable quality factor with minimum variation over a wide window of frequencies.

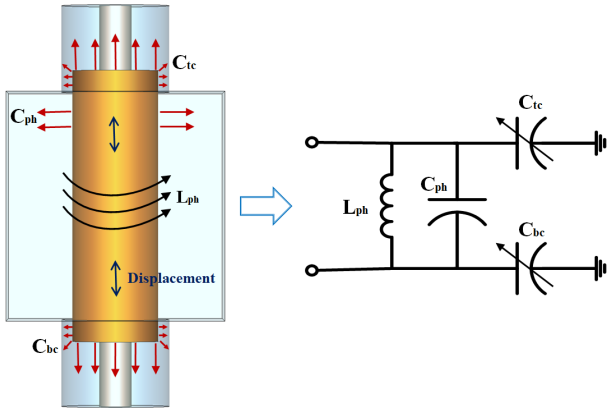

Fig. 3. Tunable inset resonator and its simplified equivalent circuit.

Through the proposal of the tunable inset resonator structure, we aim to provide a tuning mechanism that covers these stringent requirements efficiently. Fig. 3 shows a tunable inset resonator and its simplified equivalent circuit. The tuning principle is based on the displacement of the resonator to change the resonant frequency while maintaining high Q-factor without the need for additional tuning means. When the resonator is centered: this is the reference (fixed) case where the resonant frequency is the lowest. Here, the resonant frequency (f_r) can be calculated based on the corresponding inductance (L_{ph}) and total equivalent capacitance (C_T) using:

$$f_r \approx \frac{1}{2 \cdot \pi \cdot \sqrt{L_{ph} \cdot C_T}} \tag{1}$$

Where C_T comprises three main components: the capacitance between the movable inset resonator and (a) the housing (C_{ph}), (b) the top sidewall cap (C_{tc}), and (c) the bottom sidewall cap (C_{bc}):

$$C_T \approx C_{ph} + (C_{tc} \parallel C_{bc}) \tag{2}$$

Then, the tunable resonant frequency of the inset resonator can be re-expressed as:

$$f_r \approx \frac{1}{2 \cdot \pi \cdot \sqrt{L_{ph} \cdot (C_{ph} + (\frac{C_{tc} \cdot C_{bc}}{C_{tc} + C_{bc}}))}} \tag{3}$$

Moving the resonator up or down will displace it away from one sidewall cap and closer to the other sidewall end. When the resonator moves downwards, C_{tc} will decrease and the resonant frequency will move upwards with reference to the top sidewall and also, simultaneously shift down with reference to the bottom side (C_{bc} tends to increase). In general, this is correct, but due to the fact that the contained EM fields in the sidewall caps are minimal, the up-shift in the frequency caused by the displacement away from the top sidewall (C_{tc} decrease) is larger than the frequency down-shift caused by the displacement towards the opposite side inside the bottom cap (the increase due C_{bc} is comparably small and negligible). Therefore, the net result is that the resonant frequency is always shifted upwards to higher frequencies when compared to its center (fixed) state. As previously mentioned, the sidewall caps are designed to have the lowest

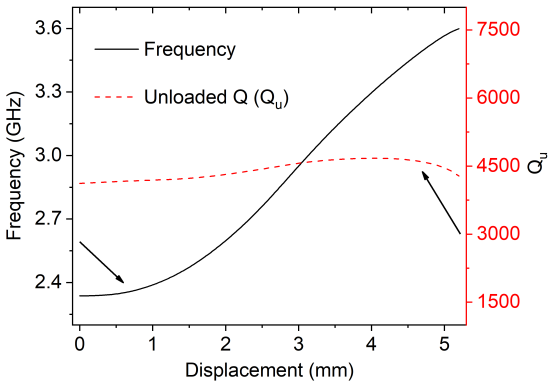

Fig. 4. Operating frequency and unloaded Q-factor in relation to the resonator displacement over the range of D=0 mm - 5.2 mm.

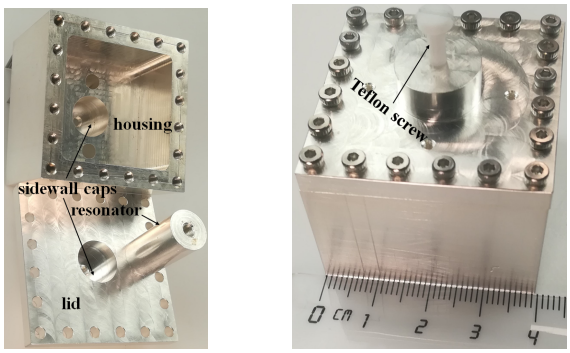

(a) (b)

Fig. 5. The fabricated tunable inset resonator prototype. (a) Disassembled and (b) assembled.

field densities. When considering the rapid decay of the EM fields, this allows designers to increase the inset-cap heights, providing further room for the movement of the resonators (hence, more tuning can be obtained) without causing any change in the reference (lowest) resonant frequency (C_{tc} and C_{bc} are fixed). Besides, since there are a small amount of fields in the caps' areas, this also means that the Q-factor will not be much affected by the tuning process, unlike what happens in most of the conventional tuning concepts. With reference to Fig. 2, the EM fields resonate as half-wavelength waves at the lower tuning states where the resonator is inserted partially at both sidewall caps. Then, the distribution of fields becomes more similar to the combline configuration at the higher tuning states where the resonator is more displaced from the first top sidewall and inserted only in the second bottom sidewall cap. Here, the electric field propagates mainly in the vicinity between the first sidewall and the resonator. In these quasi-combline cases, the Q-factor should remain stable as the resonator is not close to the top side of the housing. Another key advantage of the proposed configuration is that there is no requirement for electrical contact to the metallic cavity, contrary to the combline-based tuning concepts where excellent electrical contact is required, otherwise, both the tuning capabilities and the Q-factor will severely deteriorate.

To validate the above claims of the inset-type tuning concept, a single inset resonator example is investigated using the Eigen-mode solver in CST Microwave Studio and then manufactured and measured. Copper metal is considered in simulation for the metallic housing and resonator (electrical conductivity $\sigma = 5.8 \times 10^7$ S/m). The corresponding dimensions in (mm) are: cavity height = 15, cavity width = 30, cavity length = 30, resonator height = 20, resonator outer diameter = 10, resonator inner diameter = 3, caps height = 8, caps diameter = 11. Fig. 4 demonstrates the simulated frequency and unloaded Q-factor in relation to the resonator displacement. As shown, the frequency is reconfigured from 2.3 GHz (D=0) to 3.6 GHz (D=5.2 mm), providing a wide tunability of 44%. Additionally, the configuration has maintained a high Q_u of 4400±6.5% with minimum variation throughout the tuning window. To confirm the concept and simulation results, a prototype is manufactured and tested as depicted in Fig. 5 to Fig. 7, respectively. Each of the parts was milled out of brass metal and then silver-plated to offer high Q-factor as shown in Fig. 5. The reference state (lowest tuning state) with a wideband response was measured, as shown in Fig. 6(a). The resonator operates at 2.32 GHz with an extracted Q-factor of ≈3900 and a spurious-free band up to 3.8·f_0. The implemented resonator has a compact structure featuring a volume-saving up to 25% compared to the combline structure and 50% to the half-wavelength resonator. Fig. 6(b) demonstrates the measured tuning performance of the fabricated prototype, showing a wide frequency tuning range of 43% from 2.32 GHz to 3.59 GHz, and a stable Q_u of 4100±4% across the whole tuning window as shown in Fig. 7. These excellent results confidently validate the proposed tuning mechanism of the inset-type resonators in designing high-performance tunable filters and components. In the following section, the design procedure of constant bandwidth frequency tunable filters is explained, and different tunable inset filters are designed.

III. Tunable Inset Filters

A. Design Procedure of Tunable Filters with Constant Absolute Bandwidth

In frequency tunable filters, it is essential to maintain a constant operation bandwidth at all different frequencies within the tuning window. However, this is not easy in practice, especially when designing tunable filters with relatively wide tuning ranges (i.e. tunability >20%). To maintain a constant bandwidth response, the variation of physical inter-resonator couplings ($K_{i,j}$) and input-output couplings (Q_e) should be adjusted and balance the change in the centre frequency (f_0) as can be concluded from:

$$K_{i,j} = \frac{ABW \cdot M_{i,j}}{f_0} \tag{4}$$

$$Q_e = \frac{f_0}{ABW \cdot M_{S1}^2} \tag{5}$$

where *ABW* is the absolute bandwidth, M_{S1} and $M_{i,j}$ are the normalized coupling values, which are fixed at all frequency tuning states. Accordingly, similar to [23], the design procedure of constant bandwidth tunable filters can be formulated in three main steps as follows:

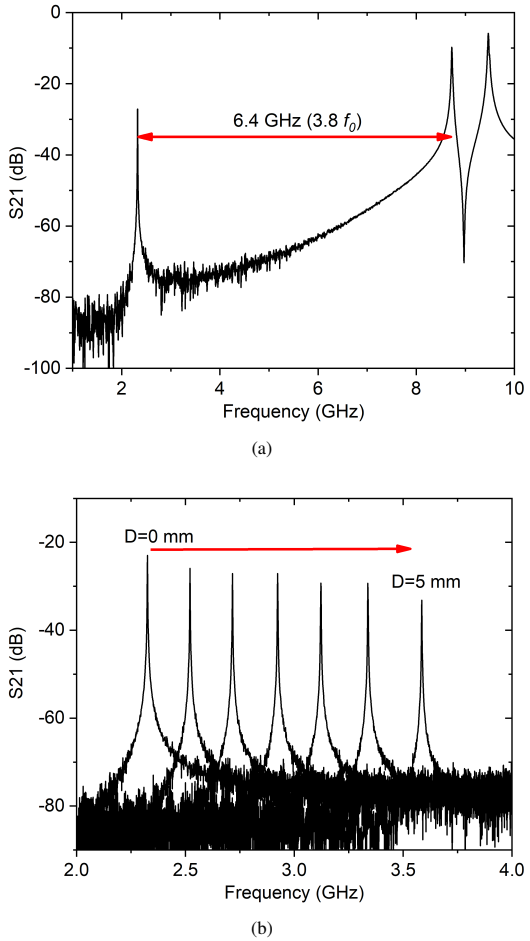

Fig. 6. Measured results of the tunable inset resonator. (a) The wideband response and (b) the tuned response over D=0 mm - 5.0 mm.

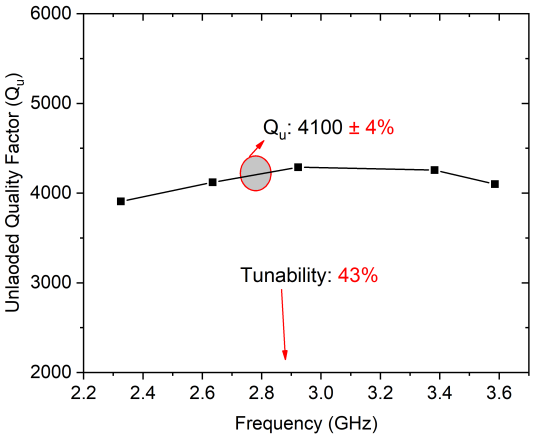

Fig. 7. Relationship between the measured Q_u of the tunable inset resonator and the tuning window of operating frequencies.

a) Extract the corresponding coupling matrix using the standard synthesis method [24] based on the desired *ABW* and other specifications.

b) From (4), and taking into account that *ABW* and $M_{i,j}$ are fixed and known from (a), the following relation must be satisfied for the required physical inter-resonator couplings ($K_{i,j}$) at every given frequency (f_n) in the tuning range:

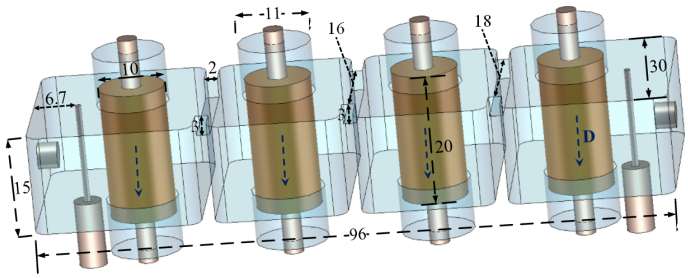

Fig. 8. 3D view of the proposed four-pole tunable inset BPF. The direction of resonators' displacement D is downwards. All dimensions are in mm unit.

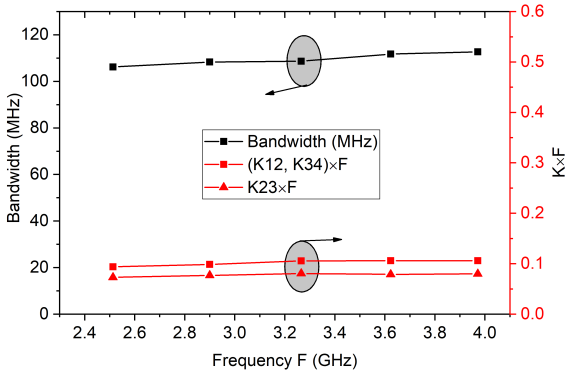

Fig. 9. Inter-resonator couplings and bandwidth variation in relation to the frequency tuning, realized through the proposed iris structures shown in Fig. 8.

$$K_{i,j} \cdot f_n = constant = ABW \cdot M_{i,j} \tag{6}$$

where the required $K_{i,j}$ is realized through the iris sections between the adjacent resonators and can be calculated as described in [24] using:

$$K_{i,j} = \frac{f_2^2 - f_1^2}{f_2^2 + f_1^2} \tag{7}$$

c) For the required input-output couplings of the CABW tunable filter: the external quality factor (Q_e) can be expressed in terms of the peak reflection group delay ($T_d(n)$) as:

$$Q_e = \frac{f_n}{ABW \cdot M_{S1}^2} = \frac{\pi \cdot f_n \cdot T_d(n)}{2} \tag{8}$$

We can then extract that:

$$T_d(n) = constant = \frac{2}{\pi \cdot ABW \cdot M_{S1}^2} \tag{9}$$

where *ABW* and M_{S1} are fixed for all tuning states and known from *step (a)*. Accordingly, the reflection group delay should be adjusted through the input feeding structure (can be extracted as explained in [24]) in order to obtain constant BWs at all tuning states.

In the following, two constant bandwidth tunable inset filters are designed based on this procedure and then implemented with two different possible control mechanisms; manually and automated motor-based setups.

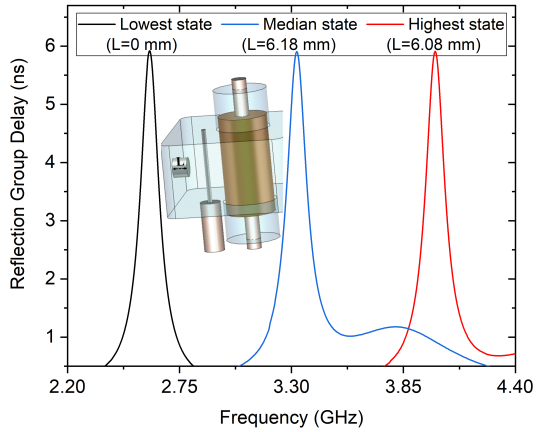

Fig. 10. Reflection group delay at the lowest, median, and highest tuning states of the filter, realized through the proposed input-feed structure shown in Fig. 8.

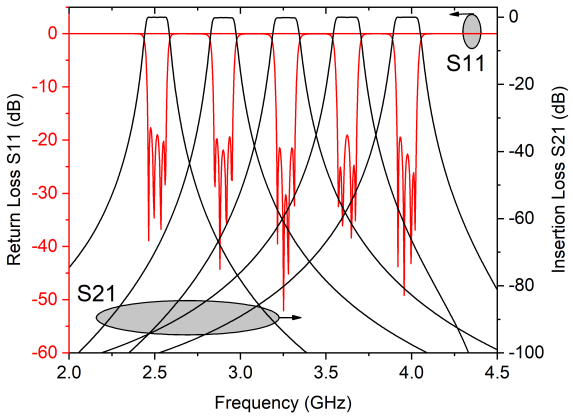

Fig. 11. Variation of the simulated S-parameters for the 4th-order tunable inset filter. The frequency is tuned from 2.54 GHz - 3.94 GHz with a CABW of 109 MHz $\pm$ 3 MHz.

B. Manually Tunable Inset Filter

Fig. 8 shows a perspective view of a four-pole inset filter. In this design, the required specifications include a wide tunability of 43% from 2.54 GHz to 3.94 GHz and a constant absolute bandwidth of 108 MHz. The desired coupling matrix is synthesized as:

$$\begin{bmatrix} & S & 1 & 2 & 3 & 4 & L \\ S & 0 & 1.035 & 0 & 0 & 0 & 0 \\ 1 & 1.035 & 0 & 0.91 & 0 & 0 & 0 \\ 2 & 0 & 0.91 & 0 & 0.70 & 0 & 0 \\ 3 & 0 & 0 & 0.70 & 0 & 0.91 & 0 \\ 4 & 0 & 0 & 0 & 0.91 & 0 & 1.035 \\ L & 0 & 0 & 0 & 0 & 1.035 & 0 \end{bmatrix}. \quad (10)$$

Then, the physical inter-resonator couplings must satisfy the following relations from (6) for all tuning states of frequency f_n (2.54 GHz – 3.94 GHz):

$$K_{12} \cdot f_n = ABW \cdot m_{12} = 0.108 \times 0.91 = 0.098 \quad (11)$$

$$K_{23} \cdot f_n = ABW \cdot m_{23} = 0.108 \times 0.7 = 0.076 \quad (12)$$

Even though further tuning elements can be added to obtain the required inter-resonator couplings (e.g. screws) of various states, this solution is unfavorable, especially in tunable filters, because it makes the tuning process more complex, very slow, and also increases the losses. Alternatively, a more suitable method can be employed is by properly designing the coupling irises to provide balanced inter-resonator couplings and maintain a constant bandwidth throughout [5], [12]. Similarly in this filter, rectangular irises (in Fig. 8) have been designed and the corresponding couplings satisfy (11) and (12), as can be seen in Fig. 9. When the filter is tuned to higher frequencies, this accordingly means that the inter-resonator couplings should decrease in a balancing manner to keep the bandwidth constant. Referring to Fig. 2, as the resonators are moving downwards, the magnetic field will tend to move towards the bottom of the cavity. Therefore, we positioned the irises at the top of the cavity, so, when the frequency is tuned up, the resonators move down, the magnetic field moves to the bottom, the inter-resonator couplings decrease, and a constant bandwidth can be obtained allover the tuning window.

Similarly, the required peak reflection group delay for a constant ABW can be calculated using (9) as:

$$T_d(n) = \frac{2}{\pi \cdot 0.108 \cdot 10^9 \cdot 1.035} = 5.7\ nS \quad (13)$$

As shown in Fig. 8, the input feeding structure is realized using 0.9 mm inductive wires through coaxial Sub-Miniature (SMA) connectors. Especially for designs with wide tuning ranges, it is convenient to introduce screws to adjust the input and output coupling strengths since only two elements are needed for any filter order. In the proposed IO feeding configuration, the IO coupling strength increases with the increase in the tunable frequency (the downwards movement of the inset resonators). Hence, two metallic M3 screws are used to decrease the

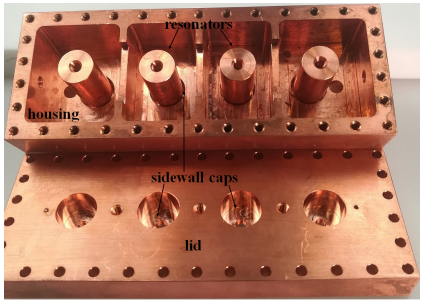

(a)

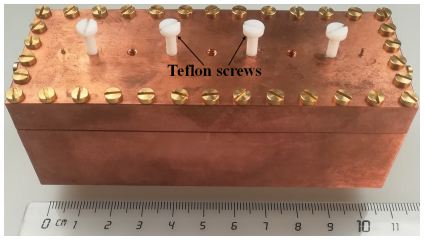

(b)

Fig. 12. The fabricated four-pole tunable inset filter. (a) Disassembled and (b) assembled.

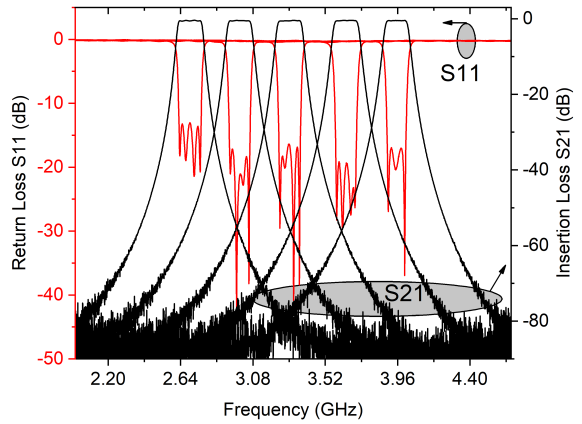

Fig. 13. Measured S-parameter results of the implemented four-pole tunable inset filter. Frequency range: 2.66 GHz to 3.96 GHz, tunability: 39.3%.

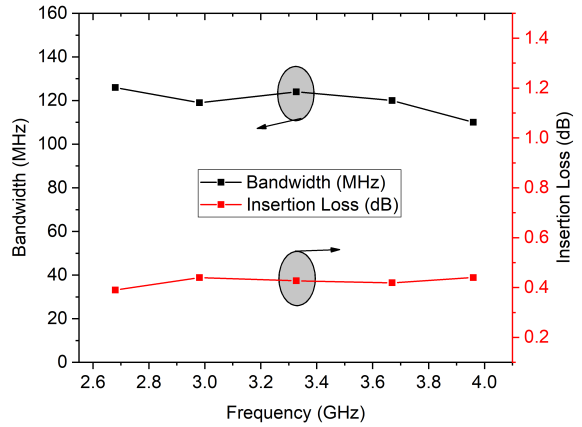

Fig. 14. Measured bandwidth (116 MHz±6%) and insertion loss response (0.39 dB - 0.44 dB) over the frequency tuning window.

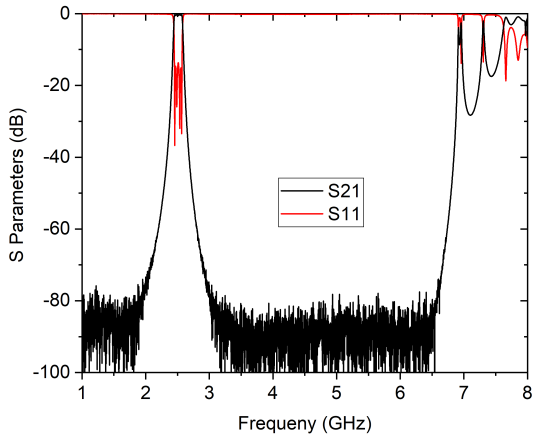

Fig. 15. Measured wideband response of the proposed four-pole inset filter's S-parameters.

IO coupling strengths with tuning, and maintain a constant reflection group delay. Fig. 10 shows the adjusted reflection group delay at the lowest, median, and highest tuning states, effectively satisfying equation (13).

A model of the filter is then designed and optimized. The simulated S-parameter responses are demonstrated in Fig. 11 at different tuning states. As shown, the filter meets the desired specifications with a constant absolute bandwidth of

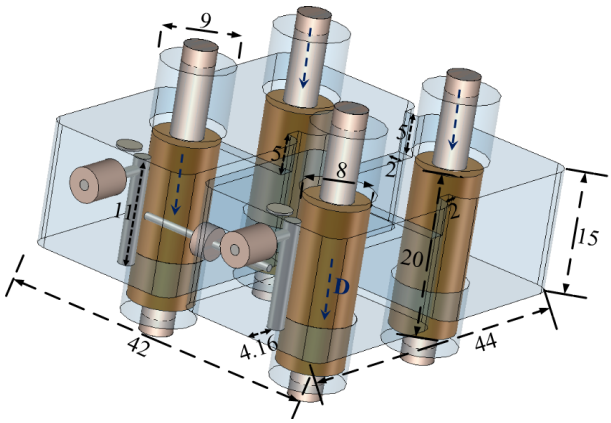

Fig. 16. 3D view of a folded four-pole tunable inset BPF. The direction of resonators' displacement D is downwards. All dimensions are in mm unit.

109 MHz ± 3 MHz and a wide tunabiltiy of 43%.

A prototype is then manufactured and assembled as depicted in Fig. 12. The filter has a compact volume of 49.28 cm^3. All parts including the resonators were milled using copper metal. 20 mm M3 Teflon screws (dielectric constant = 2.1, loss tangent = 0.0002) were used to control the displacement of the resonators inside the housing. Measurements agree very well with simulations, allowing the design procedure to be verified. The measured S-parameter responses in Fig. 13 exhibit a 1.3 GHz frequency tuning range from 2.66 GHz to 3.96 GHz with constant bandwidth of 116 MHz±6%, return loss $>$ 13.5 dB, and steady insertion loss averaging at 0.4 dB, as shown in Fig. 14. This resembles a stable Q-factor of 1820±6% throughout the 39.3% tuning window. This Q-factor corresponds to around 50% of simulated version and can be enhanced further by silver plating, similar to the earlier presented resonator prototype. Furthermore, the filter has a wide spurious-free rejection band of more than 4.3 GHz, as shown in Fig. 15. It can be noted that each of these responses was obtained effectively without the use of any tuning screws (including the IO tuners), advantageously featuring easier and faster tuning process which tracks across a wide frequency range.

Besides the presented inline all-pole filter, folded structures can be designed for the realization of cross-couplings which create transmission zeros that improve the rejection characteristics. For example, Fig. 16 demonstrates a fourth-order tunable inset filter in a quadruplet configuration with an alternative 2 mm input-feed setup to the one detailed in Fig. 8, and a capacitive probe between the source and the load to create two transmission zeros around the passband. The filter is designed similar to the earlier example and has a tuning range of 1.4 GHz and operates from 2.8 GHz to 4.2 GHz with a constant bandwidth of 77 MHz ±3 MHz, as exhibited in Fig. 17.

C. Automatically Tunable Inset Filter

In future flexible telecommunication systems (e.g. next generation satellites), the frequency bands must be remotely and automatically adjustable. Therefore, it is important to present tunable filter designs with efficient tuning techniques

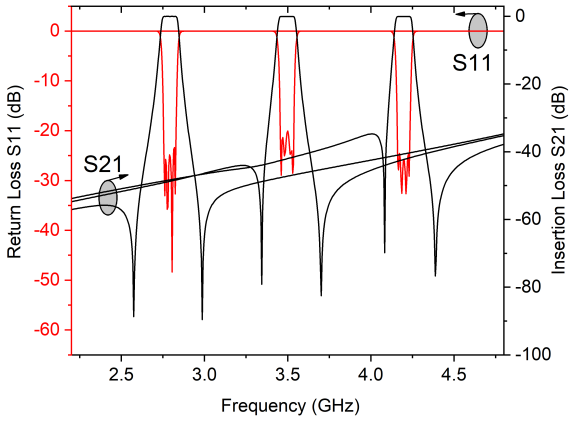

Fig. 17. Variation of the simulated S-parameters for the 4-pole tunable quadruplet inset filter. The frequency is tuned from 2.8 GHz - 4.2 GHz with a CABW of 77 MHz $\pm$ 3 MHz.

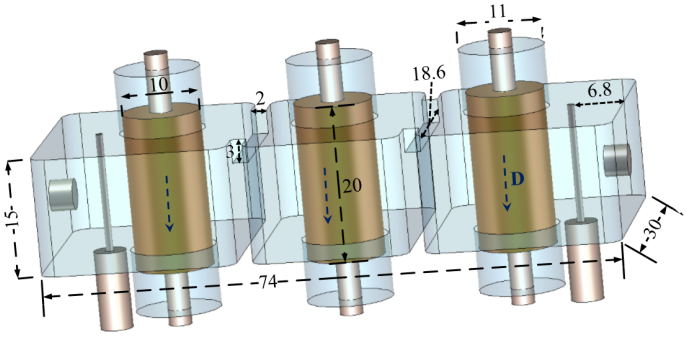

Fig. 18. 3D view of the proposed 3rd-order tunable inset BPF. The direction of resonators' displacement D is downwards. All dimensions are in mm unit.

suitable for remote tuning. The tuning mechanism should be stable, fast, and have a long-life of usage. Unfortunately, the available motorized screw-based tunable filters like [6] and [9] always need special arrangements for good electrical contact between the tuning elements and metallic housing in order to reduce the loss and prevent the leakage of radiation. This results in complex and unstable structures, having a short-life with increased losses. In contrast, the proposed contact-less inset resonator tuning concept effectively overcomes all these drawbacks and can be efficiently employed in remotely tunable designs. To validate this, a 3-pole tunable inset filter (Fig. 18) is designed and implemented in this section using pizomotors. The filter is designed to operate from 2.54 GHz to 3.96 GHz with a CABW of 102 MHz and a tunability of 43%. The design procedure is similar to the presented four-pole example. The required $k_{12} \cdot f_{\mathrm{n}}$ = 0.11 and $T_d(n)$ = 5.5 nS are calculated and then realized as shown in Fig. 19 and Fig. 20, respectively. Then, the filter model is constructed and optimized to provide the required responses. Fig. 21 exhibits the simulated S-parameters of the filter satisfying the design specifications with a 43% tunability and a CABW varying from 102 MHz to 91 MHz. Then, a copper prototype is implemented and assembled as depicted in Fig. 22 using high-accuracy LL06 piezomotors from PiezoMotor [25]. The filter has a compact size of 37.86 cm^3. A 3D-printed fixture is manufactured to properly hold the piezomotors. Here, the Teflon screws are used as posts which results in a smoother and faster

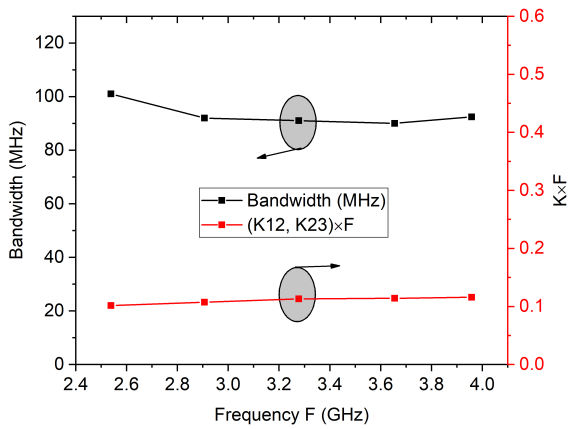

Fig. 19. Inter-resonator couplings and bandwidth variation in relation to the frequency tuning, realized through the proposed iris structures in Fig. 18.

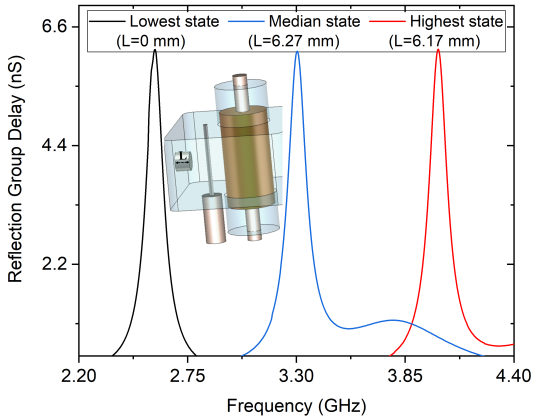

Fig. 20. Reflection group delay at the lowest, median, and highest tuning states of the filter, realized through the proposed input-feed structure shown in Fig. 18.

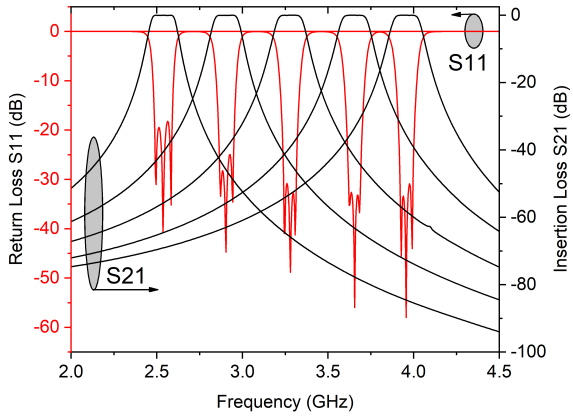

Fig. 21. Variation of the simulated S-parameters for the three-pole tunable inset filter. The frequency is tuned from 2.54 GHz - 3.96 GHz with a CABW of 96.5 MHz $\pm$ 5.7%.

tuning process, in addition to the longer usage life than the manual screw-based tuning where the Teflon material corrodes easily. The measured S-parameter responses of the fabricated filter are demonstrated in Fig. 23 with good agreement to the simulations. The filter is tuned over a 1.3 GHz window from 2.65 GHz to 3.95 GHz with a constant bandwidth of 114 MHz±8%. The filter features a return loss $>$ 15 dB, and

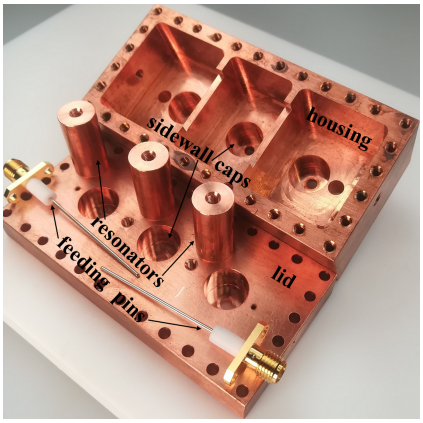

(a)

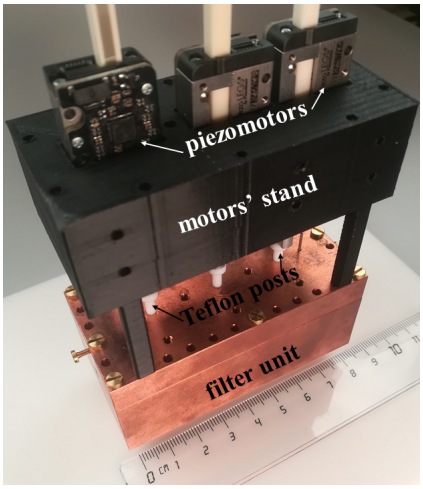

(b)

Fig. 22. The fabricated third-order filter prototype. (a) Disassembled and (b) the assembled filter unit with piezomotors.

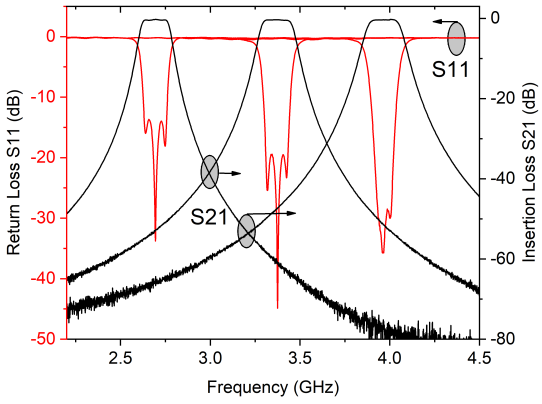

Fig. 23. Measured S-parameter results of the third-order tunable inset filter. Frequency range: 2.65 GHz to 3.95 GHz, tunability: 39.4%.

a stable insertion loss from 0.26 dB to 0.35 dB as presented in Fig. 24. Furthermore, the proposed filter has a good spurious performance better than $2.8 \cdot f_0$ as shown in Fig. 25.

IV. State-of-the-art Comparison

Table I summarizes a comparison of the presented tunable inset structures with similar CABW tunable loaded-waveguide

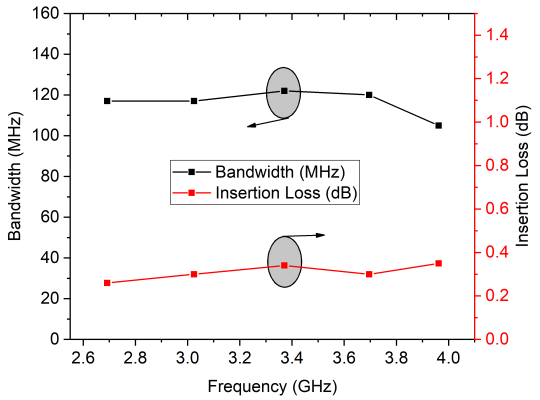

Fig. 24. Measured bandwidth (114 MHz±8%) and insertion loss response (0.26 dB - 0.35 dB) over the frequency tuning window.

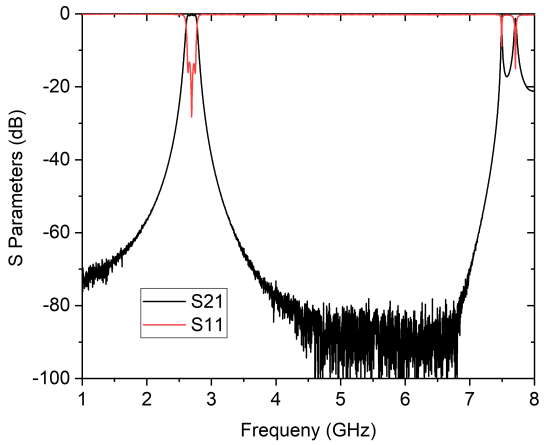

Fig. 25. Measured wideband response of the propose 3rd-order inset filter's S-parameters.

filters available in the literature. As can be seen, the tunable inset components show very competitive results including the distinctive wider tuning ranges than the other designs, and demonstrate high-Q measurements with stable performance throughout the window of tuning. In addition to these highly desirable merits, the inset components also offer more volume-saving and enhanced spurious performance (up to $3.8 \cdot f_0$). The proposed inset filters eliminate the need for any auxiliary tuning components which advantageously increases the tuning speed, reduces the losses, weight, cost, and the complexity of the tuning process. The filters have N tuning elements (which are the movable coaxial inset resonators) with two (optional) tuning elements for adjusting the IO coupling. Additionally, a mechanism of tuning using a single element can be adopted effectively using similar setups to [26] and [27], with more design effort needed for the required IO coupling, and maybe sacrificing some of the tuning range. With regard to the number of tuning elements, while we can see that the majority of designs need N independent tuning elements, the filters of [5], [7], and [12], interestingly, have a single tuning element. This provides a fast tuning feature at one side, but on the other hand, it is challenging to sustain stable and well-matched responses for the different states in the tuning window. Therefore, for practical applications,

TABLE I.
Comparison of the Proposed Tunable Inset Filters with Similar State-of-The-Art Designs

Ref.	Structure	f (GHz)	Order	Tunability (%)	ABW (MHz)	IL (dB)	Q-factor	Volume (cm^3)	Q-factor/ Volume (cm^{-3})	# Tuning Elements
[5]	Half-wavelength	2.275-2.775	4	19.8%	106.5±9%	< 0.4	$> 4850^{\ddagger}$	275.65	$> 17.6^{\ddagger}$	1
[6]	Combline-dual-post	9.15-10.87	4	17.2%	230±3.9%	< 0.6	1500	NA	NA	2N
[7]	Combline	1.81-2.17	5	18.1%	25	< 1.8	2000-2500	NA	NA	1
[8]	Dielectric-TE	15.6-16	3	2.5%	150	1.5-4.5	$421\text{-}1630^{\dagger}$	NA	NA	N
[9]	Combline	2.565-2.634	6	2.7%	NA	0.9-2.3	$2252\text{-}2914^{\dagger}$	NA	NA	N
[10]	Dielectric-combline	4.97-5.22	4	4.9%	66±1.5%	3.3-4.9	536-548	NA	NA	N
[12]	Combline	0.68-0.76	4	11.1%	11.2±8.9%	0.8-0.9	NA	2291.625	NA	1
[16]	Dual-mode dielectric-TM	4.72-5.51	2	15.4%	50±10%	0.2-0.9	540-1100	3.456	318.29	N/2
[19]	Combline	0.707-0.963	3	30.7%	27.5±2.5%	1.58-3.97	173-418	94.067	4.44	N
This work-1	Inset	2.32-3.59	-	43%	-	-	4100±4%	15.02	283.89	-
This work-2	Inset	2.65-3.95	3	39.4%	114±8%	0.26-0.35	1660±6.6%	37.86	46.74	N+2
This work-3	Inset	2.66-3.96	4	39.3%	116±6%	0.39-0.44	1820±6%	49.28	39.15	N+2

‡Based on simulated Q-factor. †Based on the measurements of a single-cavity resonator. N represents the filter order.

many designers would prefer to have independent frequency tuning elements (N), unless there is a specific need for a faster tuning process. Another comparison aspect between the different state-of-the-art designs is the tuning mechanism. For many of the mechanically tunable filters as [6] and [9], it is crucial to have a good electrical contact between the movable tuning elements and the filter cavity. Therefore, additional components are needed (e.g. nuts, elastomer, conductive ball bearings), which results in a reduced usage-life, slower tuning speed, and higher loss. Whereas the authors in [7] utilized dielectric tuners to avoid these issues, the proposed inset tuning mechanism uses freely movable contact-less resonators, similar to [5], having no requirement of any electrical contact with the cavity. It can also be noted that dielectric resonators can be used instead of metallic ones, providing more volume-saving and enhanced quality factor. This is a currently on-going research activity and will published in a future-coming article.

V. Conclusion

This work presents a new tuning technique and several tunable coaxial filters based on novel compact inset resonators. The operation principle is explained and a tunable inset resonator structure is implemented for proof-of-concept. The measured results demonstrate a wide tuning range of 43% with a stable Q-factor of 4100±4% and a wide spurious-free band up to $3.8 \cdot f_0$. A design procedure for constant bandwidth tunable filters was introduced, and two widely tunable inset filters were designed, manufactured, and measured. A manually tunable four-pole inset filter was presented featuring a frequency tuning range of 39.3%, a CABW of 116 MHz±6%, and a Q-factor of 1820±6%. Also, an automatically tunable three-pole inset filter was built to incorporate piezomotors for highly accurate and remote tuning. Similarly, the filter is demonstrated with a 1.3 GHz tuning window over the range of 2.65 GHz to 3.95 GHz with a CABW of 114 MHz±8% and a stable Q-factor of 1660±6.6% throughout the tuning window. In comparison with all available state-of-the-art loaded-waveguide CABW tunable filters demonstrated in the literature, the presented tunable inset filters provide the widest tuning ranges and the most stable performance in Q-factor. These distinctive advantages, in addition to the added benefit of compact structures and excellent spurious performance, strongly promote the proposed tuning concept for a wide range of high-performance tunable filter applications.

References

[1] *RF Tunable Filter Market*. MARKETSANDMARKETS. [Online]. Available: https://www.marketsandmarkets.com/Market-Reports/rf-tunable-filter-market-69180206.html.

[2] A. Widaa, "Comparison of Tuning Means," Report, 2020. [Online]. Available: https://ec.europa.eu/research/participants/documents/downloadPublic?documentIds=080166e5d76532fe&appId=PPGMS.

[3] A. Widaa, C. J. You and M. Awad, "High Selectivity Low-Loss Tunable Bandpass Filter with Transmission Zeros Control Using Staircase Resonators," *Proc. IEEE 18th Wireless Microwave Technol. Conf. (WAMICON)*, 2021, pp. 1-4, doi: 10.1109/WAMICON47156.2021.9443594.

[4] E. Laplanche et al., "Tunable Filtering Devices in Satellite Payloads: A Review of Recent Advanced Fabrication Technologies and Designs of Tunable Cavity Filters and Multiplexers Using Mechanical Actuation," *IEEE Microw. Mag.*, vol. 21, no. 3, pp. 69-83, Mar. 2020, doi: 10.1109/MMM.2019.2958706.

[5] G. Basavarajappa and R. R. Mansour, "Design Methodology of a High-Q Tunable Coaxial Filter and Diplexer," *IEEE Trans. Microw. Theory Techn.*, vol. 67, no. 12, pp. 5005-5015, Dec. 2019, doi: 10.1109/TMTT.2019.2937770.

[6] Y. Xie, F. -C. Chen and Q. -X. Chu, "Tunable Cavity Filter and Diplexer Using In-Line Dual-Post Resonators," *IEEE Trans. Microw. Theory Techn.*, vol. 70, no. 6, pp. 3188-3199, Jun. 2022, doi: 10.1109/TMTT.2022.3163420.

[7] M. Höft, A. Kronberger and O. Bartz, "Tunable Bandpass Filters for Multi-Standard Applications," *German Microw. Conf. (GeMiC)*, 2008, pp. 1-4.

[8] W. D. Yan and R. R. Mansour, "Tunable Dielectric Resonator Bandpass Filter With Embedded MEMS Tuning Elements," *IEEE Trans. Microw. Theory Techn.*, vol. 55, no. 1, pp. 154-160, Jan. 2007, doi: 10.1109/TMTT.2006.888582.

[9] S. Fouladi, F. Huang, W. D. Yan and R. R. Mansour, "High-Q Narrowband Tunable Combline Bandpass Filters Using MEMS Capacitor Banks and Piezomotors," *IEEE Trans. Microw. Theory Techn.*, vol. 61, no. 1, pp. 393-402, Jan. 2013, doi: 10.1109/TMTT.2012.2226601.

[10] F. Huang and R. R. Mansour, "Tunable compact dielectric resonator filters," *Proc. Eur. Microw. Conf. (EuMC)*, 2009, pp. 559-562, doi: 10.23919/EUMC.2009.5295901.

[11] M. Yu, B. Yassini, B. Keats and Y. Wang, "The Sound the Air Makes: High-Performance Tunable Filters Based on Air-Cavity Resonators," *IEEE Microw. Mag.*, vol. 15, no. 5, pp. 83-93, Jul.-Aug. 2014, doi: 10.1109/MMM.2014.2321102.

[12] G. Basavarajappa and R. R. Mansour, "A Tunable Quarter-Wavelength Coaxial Filter With Constant Absolute Bandwidth Using a Single Tuning Element," *IEEE Microw. Wireless. Compon. Lett.*, vol. 31, no. 6, pp. 658-661, Jun. 2021, doi: 10.1109/LMWC.2021.3064381.

[13] Park et al., "Variable radio frequency band filter", U.S. Patent US 7825,753 B2, Nov. 2, 2010.

[14] A. Widaa and M. Höft, "Microfluidic-Based Ultra-Wide Tuning Technique for TM010 Mode Dielectric Resonators and Filters," IEEE MTT-S Int. Microw. Filter Workshop, 2021, pp. 343-346, doi: 10.1109/IMFW49589.2021.9642347.

[15] A. Widaa and M. Höft, "A novel Re-entrant Cap Tuning Technique For TM-Mode Dielectric Resonators and Filters," *IEEE MTT-S Int. Microw. Filter Workshop*, 2021, pp. 335-338, doi: 10.1109/IMFW49589.2021.9642354.

[16] A. Widaa, C. Bartlett and M. Höft, "Miniaturized All-Reconfigurable Dual-Mode Dielectric Filter Using Piezomotors for Future Satellite Communications," *Proc. Eur. Microw. Conf. (EuMC)*, 2022, pp. 107-110, doi: 10.23919/EuMC50147.2022.9784226.

[17] A. Widaa and M. Höft, "Miniaturized Dual-Band TM-Mode Dielectric Filter and Its Reconfiguration Capabilities," *IEEE MTT-S Int. Microw. Symp. Dig.*, Jun. 2022,doi: 10.1109/IMS37962.2022.9865353.

[18] F. Huang, S. Fouladi and R. R. Mansour, "High-Q Tunable Dielectric Resonator Filters Using MEMS Technology," *IEEE Trans. Microw. Theory Techn.*, vol. 59, no. 12, pp. 3401-3409, Dec. 2011, doi: 10.1109/TMTT.2011.2171984.

[19] J. Xu, L. Yang, Y. Yang and X. Y. Zhang, "High- Q -Factor Tunable Bandpass Filter With Constant Absolute Bandwidth and Wide Tuning Range Based on Coaxial Resonators," *IEEE Trans. Microw. Theory Techn.*, vol. 67, no. 10, pp. 4186-4195, Oct. 2019, doi: 10.1109/TMTT.2019.2926251.

[20] ö. Acar, T. K. Johansen and V. Zhurbenko, "A High-Power Low-Loss Continuously Tunable Bandpass Filter With Transversely Biased Ferrite-Loaded Coaxial Resonators," *IEEE Trans. Microw. Theory Techn.*, vol. 63, no. 10, pp. 3425-3432, Oct. 2015, doi: 10.1109/TMTT.2015.2463820.

[21] A. Widaa, C. Bartlett and M. Höft, "Inset Resonators and Their Applications in Fixed/Reconfigurable Microwave Filters," *IEEE MTT-S Int. Microw. Symp. Dig.*, Jun. 2022, doi: 10.1109/IMS37962.2022.9865311.

[22] A. Widaa, C. Bartlett and M. Höft, "Tunable Resonator Arrangement, Tunable Frequency Filter and Method of Tuning Thereof", Patent pending, 2022.

[23] G. Basavarajappa and R. R. Mansour, "Design methodology of a tunable waveguide filter with a constant absolute bandwidth using a single tuning element", IEEE Trans. Microw. Theory Techn., vol. 66, no. 12, pp. 5632-5639, Dec. 2018, doi: 10.1109/TMTT.2018.2873383.

[24] R. J. Cameron, C. M. Kudsia and R. R. Mansour, Microwave Filters for Communication Systems: Fundamentals Design and Applications, Hoboken, NJ, USA:Wiley, 2018.

[25] PiezoMotor. [Online]. Available: https://piezomotor.com.

[26] Kwak et al., "variable high frequency filter device and assembly", U.S. Patent US 9,614.265 B2, Apr. 4, 2017.

[27] G. Macchiarella, L. Accatino and A. Malagoli, "Design of Ka-Band Tunable Filters in Rectangular Waveguide with Constant Bandwidth," *Proc. Asia–Pacific Microw. Conf. (APMC)*, 2020, pp. 622-624, doi: 10.1109/APMC47863.2020.9331631.

Abdulrahman Widaa (Graduate Student Member, IEEE) was born in Wad Medani, Gezira, Sudan, in 1991. He received the B.Sc. degree (Hons.) in telecommunication engineering from the University of Gezira, Wad Madani, Sudan, in 2014, and the M.Eng. degree in information and communication engineering from the University of Electronic Science and Technology of China, Chengdu, China, in 2018. He is currently working toward the Dr.-Ing. degree in electrical and information engineering with Kiel University, Kiel, Germany. From 2014 to 2016, he was a Teaching Assistant with the Electronics Engineering Department, University of Gezira. From 2016 to 2018, he was a Research Assistant with the University of Electronic Science and Technology of China, where he was involved in the design of tunable filters for RF/microwave applications. From 2018 to 2019, he was a Lecturer with the Electronics Engineering Department, University of Gezira. Since 2019, he has been an EU-Researcher with the Chair of Microwave Engineering, Kiel University, under EU Project of Advanced Technologies for future European Satellite Applications (TESLA). He was a Visiting Researcher with Technische Universität Darmstadt, Darmstadt, Germany during February–March 2020, University of Perugia, Perugia, Italy, and RF Microtech S.r.l, Italy during May–July 2021, and Universitat Politècnica de València during April–May 2022. His research interests include the design of miniaturized/tunable filters and components for microwave and satellite communications, sensors, and embedded systems. He was the recipient of many national and international awards, scholarships, and grants including the Chinese University Master Scholarship Program in 2016 and European Microwave Week Student Grant in 2020 and 2021, respectively.

Chad Bartlett (Graduate Student Member, IEEE) was born in Nelson, BC, Canada, in 1987. He received the B.Eng. and M.A.Sc. degrees in electrical engineering from the University of Victoria, Victoria, BC, in 2017 and 2019, respectively. He is currently pursuing the Dr.-Ing. degree at the Chair of Microwave Engineering, Department of Electrical and Information Engineering, Kiel University, Kiel, Germany. His primary research interests include microwave and millimeter-wave passive components, filters, and antenna networks for the next generation of satellite and communication systems, as well as developing methods for overcoming challenges in micro-scale designs. Mr. Bartlett is a member of the European Union's Horizon 2020 research and innovation program for early-stage researchers.

Michael Höft (Senior Member, IEEE) was born in Lübeck, Germany, in 1972. He received the Dipl.-Ing. degree in electrical engineering and the Dr.-Ing. degree from Hamburg University of Technology, Hamburg, Germany, in 1997 and 2002, respectively. From 2002 to 2013, he joined the Communications Laboratory, European Technology Center, Panasonic Industrial Devices Europe GmbH, Lüneburg. He was a Research Engineer and then the Team Leader, where he had been engaged in research and development of microwave circuitry and components, particularly filters for cellular radio communications. From 2010 to 2013, he was the Group Leader of research and development of sensor and network devices. Since October 2013, he has been a Full Professor with the Faculty of Engineering, Kiel University, Kiel, Germany, where he is the head of the Chair of Microwave Engineering, Department of Electrical and Information Engineering. His research interests include active and passive microwave components, submillimeter-wave quasioptical techniques and circuitry, microwave and field measurement techniques, microwave filters, microwave sensors, and magnetic field sensors. Dr. Höft is a member of the European Microwave Association (EuMA), the Association of German Engineers (VDI), and the German Institute of Electrical Engineers (VDE).